AN ABSTRACT OF THE THESIS OF

Hsuan-Yu Leu for the degree of Master of Science in Chemical Engineering presented on November 20, 2014.

Title: Spray Drying for Erythrocyte Preservation at Room Temperature

Abstract approved:

Adam Z. Higgins

Spray drying has been widely used in food science for long-term storage of products such as powdered milk, and it has recently been used for preservation of more temperature sensitive products such as human blood plasma and single-cell organisms. However, there are no previous reports of successful spray drying of viable mammalian cells. This study lays the groundwork for spray drying of red blood cells (RBCs), with the ultimate goal of creating a blood transfusion product that is stable at room temperature.

To identify promising operating conditions for RBC spray drying, experiments were performed to measure the moisture sorption characteristics of RBCs, as well as their sensitivity to thermal damage. The moisture sorption isotherm of packed RBCs was measured by equilibrating the sample in various relative humidity environments and measuring the residual moisture content. The resulting data was sigmoidal in shape, in agreement with the best-fit Guggenheim–Anderson–de Boer (GAB) model. RBC sensitivity to thermal damage was determined by measuring hemolysis and cell recovery after exposure to temperatures between 37 °C and 80 °C for 25 s. There was no apparent damage for temperatures up to 60 °C, but exposure to temperatures of 70 °C or higher caused complete cell lysis. Together, the results of these experiments

allowed the use of a mathematical model of the spray drying process to identify promising operating conditions.

Based on these model predictions, preliminary RBC spray drying experiments were performed using a custom system consisting of a two-fluid atomizer, a drying chamber and a biosafety enclosure with a HEPA filter. The results demonstrate the potential for creation of an RBC powder that is sufficiently dry for long term storage. However, few intact RBCs were observed after rehydration. To improve RBC viability, we suggest that the spray drying system should be modified to enable a secondary gas input and better insulation of the drying chamber.

Spray Drying for Erythrocyte Preservation at Room Temperature

by
Hsuan-Yu Leu

A THESIS

submitted to

Oregon State University

in partial fulfillment of
the requirements for the
degree of

Master of Science

Presented November 20, 2014
Commencement June 2015

Master of Science thesis of Hsuan-Yu Leu presented on November 20, 2014

APPROVED:

Major Professor, representing Chemical Engineering

Head of the School of Chemical, Biological, and Environmental Engineering

Dean of the Graduate School

I understand that my thesis will become part of the permanent collection of Oregon State University libraries. My signature below authorizes release of my thesis to any reader upon request.

Hsuan-Yu Leu, Author

ACKNOWLEDGEMENTS

First of all, I would like to express my deepest gratitude to my family, my parents Booky and Fenny, my litter sister Joy, and my fiancé Jin. Without your support, there is no way for me to study abroad. I would also like to thank my advisor, Dr. Adam Higgins. Thanks for giving me guidance throughout the experimental detail and equipment design. Especially during the thesis revision, your patience still impressed so much. Auxiliary was provided from Bronson Ayala and 2012 senior project team for assisting preliminary studies, Dr. Karl Schilke for borrowing the drying oven in his lab, and Emma Burgess and Andy Brickman for helping the enclosure installation.

CONTRIBUTION OF AUTHORS

Dr. Adam Z. Higgins assisted with the guidance of the development and planning of experiments, building up the spray drying enclosure, as well as the editing and finalization of this thesis.

TABLE OF CONTENTS

TABLE OF CONTENTS (Continued)

LIST OF FIGURES

LIST OF TABLES

Spray Drying for Erythrocyte Preservation at Room Temperature

CHAPTER 1: Introduction

1.1 Present Blood Supply Chain

In 2011, more than 13 million units of blood were transfused in the United States alone, according to the National Blood Collection and Utilization Survey Report. As a result of the short storage life of conventionally stored blood, and the high demand for transfusions, new technologies for stable long-term blood storage are being rapidly developed. Current techniques can store blood in the refrigerated state for up to 6 weeks without compromising viability or causing adverse physical responses in the recipient upon transfusion. Seasonal shortages did occur, even though those were rare [1]. To avoid shortages, techniques for the cryopreservation of blood, which can extend the shelf life for up to ten years, have been developed. Moreover, post-thaw analysis for cryopreserved RBCs has shown favorable cell recovery [2, 3]. But before administration, cryopreserved RBCs must be deglycerolized which takes approximately an hour [4]. The amount of time needed to make the RBCs ready for transfusion prevents a timely and effective administration during certain emergency situations. Besides the inconvenience of the post-thaw process, the cost of the maintenance of cold chain is a significant issue as well. In certain situations, such as in an active war zone, or after an earthquake, tsunami, or a hurricane, electricity outages would make it impossible to sustain the cold chain. Therefore, we propose to develop a process capable of spray drying RBCs for storage at room temperature.

1.2 Requirements for Room Temperature Storage of RBCs

In order to successfully preserve erythrocytes at room temperature, one must take steps to ensure long-term stability during storage. This can be understood in terms of the glass transition temperature, a concept that may be more familiar in the context of polymer processing. In polymers, rubber-like behavior appears when the surrounding temperature (T) is greater than glass transition temperature (T_g). Rubber-like behavior shows high mobility, but when mobility is high, so is the risk of damage to the cell. In contrast, $T < T_g$ leads to glassy behavior, which decreases the risk of damage to the cell. In other words, if the T_g of RBC is greater than room temperature (T_{room}), then the RBC is in a glassy state and the chance of cell damage is lower. In essence, the higher the T_g, the wider the range of temperature in which we can keep the cell stable and relatively safe from damage. Generally speaking, T_g is related to the amount of plasticizer in the polymer; the less the plasticizer, the higher the T_g. In cells, water is analogous to the plasticizer in polymers: the less the water content, the higher the T_g, and the greater the range of temperature in which the cell can be kept stable.

1.3 Freeze Drying and Spray Drying

Increasing T_g means reducing the water content of RBCs (desiccating the RBCs). Freeze drying and spray drying are two commonly studied methods to achieve room temperature storage. Freeze drying RBCs for room temperature preservation is a topic of current research, [5, 6] but spray drying has only been applied to human blood plasma [7] and some single-cell organisms [8, 9]. Even though the method of freeze drying has been applied to RBCs, cell recovery was unacceptably low [5, 6]. Past

studies have shown that multiple types of damage occur during the lyophilization process: Kanias and Acker found oxidative damage of hemoglobin induced from the desiccating process [10], and Torok et al. found membrane damage by observing the morphology of the RBCs under SEM [6].

Recent studies have shown that desiccation damage to mammalian cells is time-dependent [11, 12]. Typically the freeze drying process takes over 10 hours from beginning to end, at which point the RBCs can theoretically be stored at room temperature. Spray drying of RBCs has the potential to reduce desiccation damage to the cell because of the quick drying time. The RBC solution is atomized at the nozzle and then desiccated by the surrounding heated dry gas. Generally, spray drying is accomplished in seconds [13], which is 4 orders of magnitude faster than freeze drying. Because of this, spray drying seems like an attractive alternative because of potential for mitigation of desiccation damage due to reduced drying time.

1.4 Mechanisms of Damage

The spray drying process can cause damage to the RBCs as a result of RBC dehydration, the surrounding hot gas can induce hyperthermia damage, and the atomization process itself can result in shear damage. The advantage of spray drying however is the quick drying time – tiny droplets containing RBCs are generated by atomization, and are quickly dried by the surrounding hot gas.

1.4.1 Dehydration Damage

According to the Kanias and Acker study, hemoglobin is oxidized as a result of the desiccation process [10]. Trehalose, a popular lyoprotectant, has shown its ability to stabilize intracellular proteins and thus intracellular structure due to it's ability to hydrogen bond [14]. Not only does trehalose have a capability to protect the cell, but it also happens to have a relatively high T_g. Because of this, the T_g for an RBC loaded with trehalose is expected to be higher than that of an RBC not loaded with trehalose. The higher T_g makes it possible to achieve the same cell stability, but with a higher moisture level (thereby reducing damage from dehydration). Thus, introducing trehalose into RBCs mitigates the dehydration damage and at the same time elevates the threshold of the maximum water content in the RBCs.

1.4.2 Hyperthermia Damage

It is important to note that a liquid water jacket encompasses each RBC droplet when the droplet is formed. As the result, the RBC will be at a lower temperature than the drying gas because of the cooling effect of evaporation of the liquid jacket. Consequently, the wet-bulb temperature estimates the temperature experienced by the RBC.

Most of the previous studies involving hyperthermia and RBCs have shown that temperature-induced hemolysis increases significantly when the temperature increases above 62°C [15-17]. In those previous studies however, the RBCs were slowly subjected to the elevated temperatures for minutes or hours, which doesn't properly simulate the process of spray drying, which involves a very rapid

temperature increase that only lasts, at the most, seconds. Fildes et al. found that RBCs could tolerate up to a 60°C heat-shock for 0.6 or more seconds without causing significant hemolysis and osmotic fragility [18]. Short lasting hyperthermia exposure, lasting seconds rather than minutes or hours, more closely simulates the conditions that the RBCs are exposed to during spray drying.

In previous studies, conventional lyoprotectants such as glycerol [19, 20] and sorbitol [21] have been shown to protect RBCs against hyperthermia damage. From this we can reason that trehalose, another conventional lyoprotectant, may also strengthen RBC tolerance to high temperatures.

1.4.3 Shear-Induced Damage

Several types of atomizers were introduced in the Spray Drying Handbook: rotary, pressure, two-fluid, and ultrasonic atomizers [22]. Our preliminary study has focused on the shear-induced damage to RBCs from a two-fluid atomizing nozzle. Shear damage was decoupled from other mechanisms of cell damage by using un-heated humid nitrogen for the atomizing gas. According to the McLean et al. study, RBC hemolysis is highly related to the hematocrit of the solution and to the liquid to gas flow rate ratio [23]. In their study they showed that shear-induced hemolysis could be diminished to less than 5%. We can therefore design our experimental parameters after their study to minimize the shear-induced damage during spray drying.

1.5 Study Overview

In this study, we started by identifying favorable output conditions for RBC spray drying. We estimated an acceptable range for T_g and the corresponding moisture content in the dried RBC powder by finding the moisture sorption isotherm. We also found a favorable output temperature by investigating the temperature threshold for hyperthermia damage to RBCs. In addition to identifying these target outlet conditions, we also determined the extent of damage during the trehalose-loading process by observing the stability of trehalose-loaded RBCs. Next, a mathematical model was constructed using this information. The mathematical model suggested operating parameters for the RBC spray drying experiment. The experimental data collected during RBC spray drying was compared to the predicted results from the mathematical model. Additionally, the dried RBC powder was observed under the microscope to qualatively test the RBC product for the appearance of viability.

CHAPTER 2: Materials and Methods

2.1 Mathematical Model of Spray Drying Process

To facilitate selection of operating conditions for RBC spray drying, a mathematical model was developed based on conservation of mass and energy. The spray drying process is illustrated schematically in Fig. 1. Drying gas and a liquid feed containing RBCs are fed to the drying chamber, where the liquid is atomized into tiny droplets.

Within the drying chamber water evaporates from the liquid droplets, resulting in a dry powder and humid gas at the outlet. To develop a mathematical model of this process we assumed isobaric steady-state conditions within the drying chamber and thermal and chemical equilibrium between the dried powder and humid gas at the drying chamber outlet.

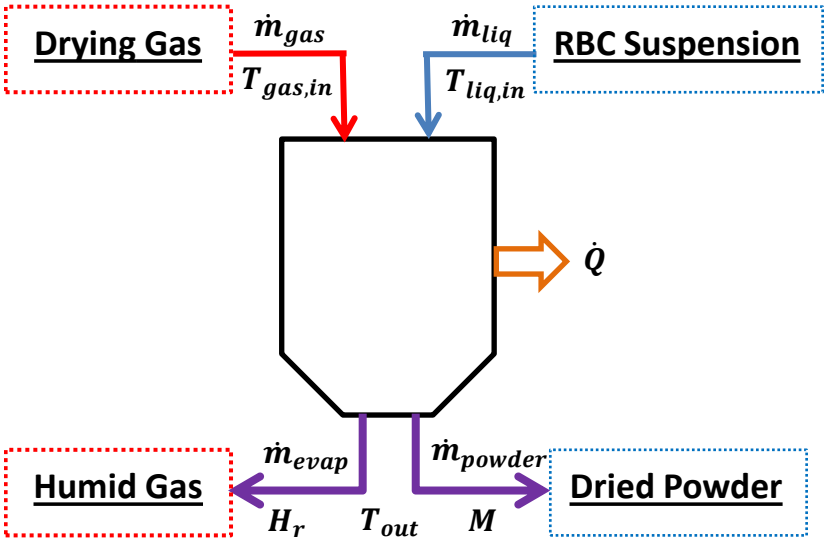

Fig.1 Control volume for mathematical model of the spray drying process.

To relate the relative humidity at the drying chamber outlet to the moisture content in the dried RBC powder, we used the Guggenheim–Anderson–de Boer (GAB) model:

$$M = \frac{100 M_m C K H_r}{(100 - K H_r)[100 + (C - 1) K H_r]} \qquad 1$$

where M is the dry basis moisture content, H_r is the relative humidity, and M_m, C and K are constants characterizing the moisture sorption properties of the material. This

model is commonly used to describe the moisture sorption properties of foods [28], and it has also been used for biological cells, including yeast [29] and platelets [30].

The mass flow rate of RBC powder (which contains both residual water and solid components) can be expressed in terms of the dry basis moisture content (M) and the mass flow rate of solids as follows:

$$\dot{m}_{powder} = (1 + M) x_{solids} \dot{m}_{liq} \quad (2)$$

where x_{solids} is the mass fraction of solids in the liquid feed and $\dot{m}_{liq}$ is the liquid feed mass flow rate.

The powder flow rate can then be used to calculate the rate at which water evaporates in the drying chamber:

$$\dot{m}_{evap} = \dot{m}_{liq} - \dot{m}_{powder} \quad (3)$$

The rate of evaporation can be used to determine the water content of the exiting gas stream, which can be expressed in terms of relative humidity as follows:

$$H_r = 100 \left(\frac{P}{P^*}\right)\left(\frac{\dot{m}_{evap}/W_w}{\dot{m}_{evap}/W_w + \dot{m}_{gas}/W_{gas}}\right) \quad (4)$$

where P is the absolute pressure in the drying chamber (assumed atmospheric), P^* is the equilibrium vapor pressure of water at T_{out} and W_w and W_{gas} are the molecular

weights of water and the drying gas, respectively. To account for the temperature dependence of P^*, we used the Antoine equation:

$$log_{10}P^* = A - \frac{B}{T_{out} + C} \quad (5)$$

where *A*, *B* and *C* are published constants [31], T_{out} is in Celsius and P^* is in mmHg.

An energy balance on the drying chamber consists of the energy lost by the drying gas, the energy gained by the liquid and energy lost as heat:

$$\dot{m}_{gas}\int_{T_{gas,in}}^{T_{out}} C_{p,gas}dT + \dot{m}_{liq}\int_{T_{liq,in}}^{T_{out}} C_{p,liq}dT + \dot{m}_{evap}\Delta\hat{H}_v + \dot{Q} = 0 \quad (6)$$

where $\dot{m}_{gas}$ is the mass flow rate of the drying gas; $T_{gas,in}$ and $T_{liq,in}$ are the inlet temperatures of the gas and liquid feeds, respectively; $C_{p,gas}$ and $C_{p,liq}$ are the heat capacities of the gas and liquid feeds, respectively; $\Delta\hat{H}_v$ is the heat of vaporization of water at the outlet temperature T_{out}; $\dot{Q}$ is the heat. The temperature dependence of the heat of vaporization was estimated using a linear fit to published data [31] over the temperature range 2°C to 102°C, resulting in:

$$\Delta\hat{H}_v = -2.4453 * T_{out} + 2503.6 \quad (7)$$

where $\Delta\hat{H}_v$ is in kJ/kg and T_{out} is in Celsius.

Together, these equations allow calculation of the properties of the RBC powder at the drying chamber outlet as a function of the following key process parameters: $\dot{m}_{liq}$, x_{solids}, $\dot{m}_{gas}$, $T_{liq,in}$, $T_{gas,in}$ and $\dot{Q}$. Alternatively, the equations can be used to identify combinations of process parameters that result in desired outlet conditions, such as a temperature low enough to avoid thermal damage and a moisture content low enough to ensure stability during storage. The equations were solved simultaneously using a custom MATLAB program.

2.2 Isolation of RBCs

Human whole blood was either purchased from BioreclamationIVT (Baltimore, MD) or collected by venipuncture from volunteer donors using an IRB approved protocol. The blood was refrigerated in tubes containing citrate, phosphate, and dextrose (CPD) as an anticoagulant for up to 14 days. Immediately before using the cells in experiments, the RBCs were isolated by centrifuging the sample at 1200 g for 5 min, discarding the supernatant and resuspending the sample in isotonic phosphate buffered saline (PBS) solution (142 mM sodium chloride, 12.5 mM disodium phosphate, 11.1 mM glucose, pH 7.2). This PBS wash process was repeated 3 times.

2.3 Moisture Sorption Isotherm

The equilibrium moisture content of partially dried RBCs was measured under a range of relative humidity conditions to create a moisture sorption isotherm. Saturated salt solutions were used to generate a controlled relative humidity environment [30], as illustrated in Fig. 2. Six different relative humidity conditions were prepared using the following salts at 25± 1 °C: lithium bromide (LiBr), lithium chloride (LiCl), potassium acetate (CH_3CO_2K), magnesium nitrate ($Mg(NO_3)_2$),

potassium carbonate (K_2CO_3), and sodium chloride (NaCl). A small volume (250 µL) of packed RBCs in a plastic weigh boat was placed on top of the saturated salt solution within a sealed Mason jar. After 1 week, the RBC sample was removed from the Mason jar for assessment of residual moisture content. Two different drying conditions were examined for removal of residual moisture from the RBC sample: 150 °C for 3 ± 0.5 h and 105 °C for 23 ± 1 h. The dry basis moisture content was determined by comparing the initial sample mass to the final sample mass after drying in the oven. As an assay control, we measured the moisture content of sodium tartrate, which exists as a dihydrate crystal with dry basis moisture content of about 18.6% [32]. All experiments were performed in triplicate. To quantitatively characterize the relationship between moisture content and relative humidity, the data was fit using the GAB model (Eq. 1) using a least squares method.

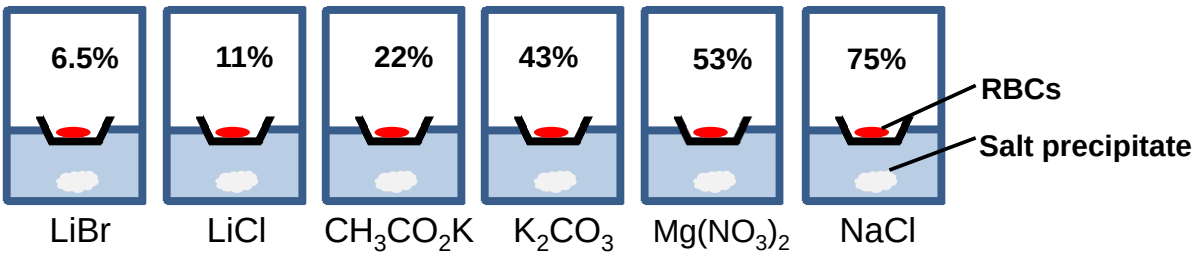

Fig. 2 Relative humidity conditions for determining moisture sorption isotherm. Six different saturated salt solutions were used to generate the indicated relative humidity values.

2.4 RBCs Sensitivity to Elevated Temperatures

To evaluate the potential for thermal damage, RBCs were exposed to a range of temperatures for 25 ± 5 s and then returned to physiologic temperature (37 °C). The desired temperature was achieved by mixing 100 µL of 40% hematocrit RBC

suspension with 3.9 mL of heated PBS, and placing the resulting mixture in a heated water bath until the total exposure time reached 25 s. At that point, the sample temperature was returned to 37 °C by addition of an appropriate volume of chilled (0 °C) PBS. The exposure temperatures and corresponding solution volumes are given in Table 1.

Table 1. RBC exposure temperature and volume of chilled PBS added to return the sample to 37 °C.

Exposure Temperature (°C)	Volume Pre-Chilled PBS (0°C) Required (mL)
37	0
45	0.865
50	1.41
55	1.95
60	2.49
65	3.03
70	3.57
80	4.65

Thermal damage to the RBCs was assessed by measuring cell recovery and hemolysis. Cell recovery was quantified by counting intact cells on a hemacytometer; percent recovery was calculated by normalizing to the control sample (i.e., 37 °C exposure temperature). To determine hemolysis, the amount of free hemoglobin in the sample was quantified using Harboe's direct spectrophotometric method [33] and normalized to a 100% lysis control, as described in our previous study [34].

Because elevated temperatures can cause hemoglobin aggregation [35] – which may interfere with detection of free hemoglobin and consequently impact hemolysis measurements – we performed control experiments in which the RBCs were exposed to elevated temperatures in the presence of pure water. The experimental conditions

were identical to those described above, except that the cells were brought to the desired elevated temperature by addition of heated water and returned to 37 °C by addition of chilled water. Under these conditions all of the RBCs would be expected to swell and lyse, releasing their hemoglobin into the supernatant.

2.5 Stability of Trehalose-Loaded RBCs

Trehalose loading was performed as described previously [26]. Packed RBCs were brought to 30% hematocrit using trehalose loading buffer (800 mM trehalose, 6.7 mM phosphate, 24.0 mM glucose, 0.433 mM adenine, 33.3 mM NaCl, and 8.87 mM mannitol at pH 7.2) and incubated at 37 °C for 7 h. The RBCs were then washed twice with PBS and stored at 4 °C for various times to assess the stability of the cells after trehalose loading. The hemoglobin content was quantified in the supernatant from the two PBS washes, as well as the supernatant of the sample after 4 °C storage, using the spectrophotometric method described above. The sum total hemoglobin content was compared to a 100% lysis control to determine the percent hemolysis.

2.6 Spray Drying of RBCs

The spray drying system is shown in Fig. 3. It consists of a cylindrical drying chamber within a sealed biosafety enclosure. Ports at the top of the biosafety enclosure allow introduction of liquid and gas feeds. These feed streams are then fed to a two-fluid atomizer nozzle (1/4J SS nozzle body, 1650 fluid cap, 1153-64 air cap, Spray Systems Co., Wheaton Illinois) located at the top surface of the drying chamber. The nozzle generates a mist within the drying chamber, which is converted to a dried powder as water evaporates from the droplets. At the drying chamber outlet, the

powder is collected onto filter paper (Grade GF/D, Whatmann), while the gas passes through the filter paper and into a piping system that leads to a fume hood. The piping system includes a HEPA filter to decontaminate the gas stream, and a duct fan to draw the gas through the pipes. An opening in the piping system was also included to allow decontamination of the air in the biosafety enclosure. This air is drawn into the piping system and through the HEPA filter by the duct fan. To allow intake of clean air into the enclosure, 0.2 μm filters were integrated into one of the enclosure walls.

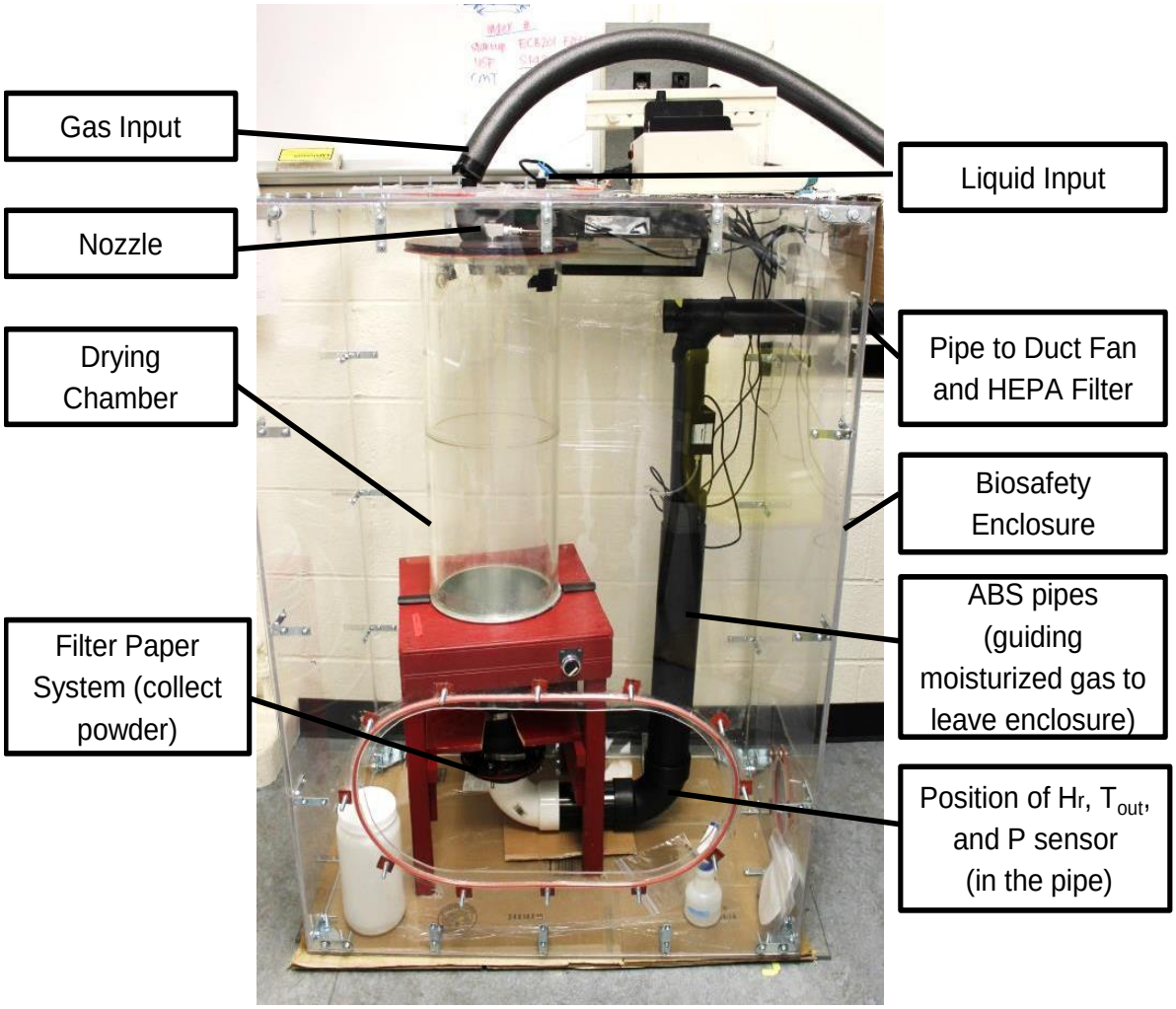

Fig. 3 Description of Spray Drying System

The biosafety enclosure includes 3 ports that allow access to the interior: a top port that allows removal of the drying chamber (if necessary), a front port where gloves can be mounted, and a side port for introduction and removal of samples. During operation of the spray dryer these ports were covered and sealed with O-rings to prevent escape of potentially infectious particulates into the room. After completion of drying, the filter paper and dried powder was removed from the piping system using the gloves mounted to the front of the enclosure, and placed into a sealed Ziploc bag. Fig. 4 illustrates how the filter paper was integrated into the piping system. The filter paper was compressed between two flanges, which were tightened together using bolts and wing nuts. Stainless steel mesh was placed below the filter paper to provide structural support. After placing the sample in the Ziploc bag, the duct fan was run for 30 minutes to decontaminate the air in the enclosure, and the sample was removed through the side port for further analysis.

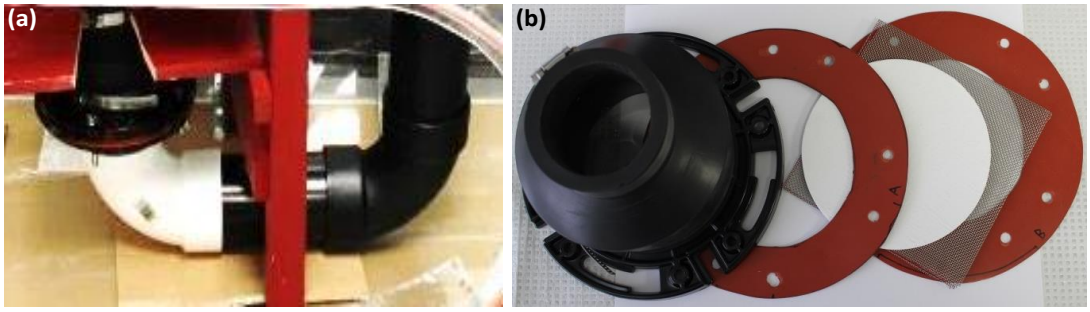

Fig. 4 Spray drying filter paper system. (a) Zoom in image of the filter paper system from the whole spray drying system. (b) Composition of the filter paper system (from left to right) – top toilet flange, top rubber disk, filter paper, stainless steel mesh, and bottom rubber disk.

The mathematical model of the spraying process (Eqs. 1-7) was used to identify promising conditions for RBC spray drying. The inlet conditions required for the model were measured as follows. The mass flow rate of the liquid feed ($\dot{m}_{liq}$) was determined by multiplying the volumetric flow rate (as determined using the syringe pump; see Fig. 5a) by the solution density. The solution density ρ was calculated as a function of hematocrit (*Hct = 0.05*) as follows:

$$\rho = (Hct)\rho_{RBC} + (1 - Hct)\rho_{PBS} \quad (8)$$

where ρ_{RBC} = 1.125 g/mL is the density of RBCs [36] and ρ_{PBS} = 1 g/mL is the density of PBS. The mass fraction of solids in the liquid feed (x_{solids}) was also calculated as a function of hematocrit:

$$x_{solids} = (Hct)\left(\frac{\rho_{RBC}}{\rho}\right)x_{RBC} \quad (9)$$

where x_{RBC} = 0.35 is the solids fraction of normal RBCs [37]. To determine the mass flow rate of nitrogen gas fed to the atomizer ($\dot{m}_{gas}$), the volumetric flow rate from the rotameter (see Fig. 5b) was corrected for the deviation from standard temperature and pressure using the manufacturer's instructions. The gas temperature was measured using a thermocouple taped to the outside of the tube flowing into the rotameter, and the pressure was estimated using the gas regulator. After the rotameter, the gas was fed to a copper coil immersed in a heated ethylene glycol and water mixture solution (Fig. 5c). To determine $T_{gas,in}$ the tube running from the heated bath to the biosafety

enclosure was disconnected and a thermocouple was placed into the tube outlet; this allowed estimation of the temperature just upstream of the atomizer. The liquid temperature at the inlet to the atomizer ($T_{liq,in}$) was measured in a similar fashion.

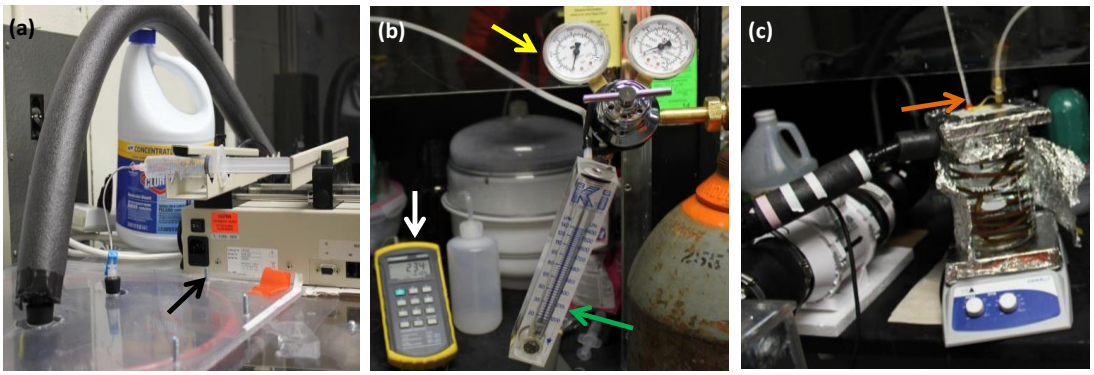

Fig. 5 Spray drying input parameters. (a) Liquid compressed by syringe pump (black arrow). (b) Gas compressed by gas tank; the needed parameters to determine the mass flow rate of nitrogen gas: the volumetric flow rate from rotameter (green arrow), temperature from thermocouple (white arrow), pressure from regulator (yellow arrow). (c) Input gas heated by ethylene glycol solution, temperature from thermometer (orange arrow).

Prior to starting each spray drying experiment, nitrogen gas was fed to the drying chamber in order to remove moisture from the system and help achieve thermal equilibrium. The nitrogen gas was heated to an inlet temperature of at least 85 °C and fed at 30 g/min for at least an hour. The liquid feed was initiated once the relative humidity measured at the drying chamber outlet was less than 5%.

Powder rehydration and residual moisture content were the two tests in order for us to understand how well our system works. Powder, originally on the filter paper, was scratched down to the same Ziploc bag. A small amount of powder (15 mg) was rehydrated with PBS and observed under the microscope with a hemacytometer. The other small amount of powder (25 mg) was used for detecting the residual moisture

content (in the same manner as moisture sorption isotherm experiment). Powder collection, powder rehydration, and powder residual moisture content detection were all manipulated in a biosafety cabinet. This study has done two batches of blood for spray drying; in each batch, there were two replicates in the rehydration test but only one in the residual moisture content test.

2.7 Statistical Analysis

Results are reported using the mean and standard error of the mean. Each replicate was obtained using a different batch of blood. The data was analyzed using ANOVA with batch of blood used as a blocking factor; Fisher's least significant difference (LSD) test was used for pairwise comparisons. Differences were defined to be statistically significant at the 95% confidence level. All analysis was performed using StatGraphics software.

CHAPTER 3: Results

3.1. Mathematical Model of the Spray Drying Process

The ultimate goal of this research is to develop a spray drying method that enables long term storage of viable RBCs in a dried state. Spray drying is a complex process with many interacting process parameters that are challenging to optimize empirically [38, 39]. Therefore, we sought to leverage mathematical modeling based on mass and energy balances to identify promising regions of the operating space for RBC spray

drying. Fig. 3 illustrates how the mathematical model can be used to guide selection of process parameters. The goal of spray drying is to achieve a sufficiently dry powder for long term storage. To this end, the model can be used to define process parameters that achieve a target moisture content (M) in the dried powder, as shown in Fig. 3. The target moisture content is achieved for specific combinations of feed flow rates ($\dot{m}_{liq}/\dot{m}_{gas}$) and drying gas temperature ($T_{gas,\ in}$). A subset of those conditions would be expected to cause thermal damage to the RBCs, allowing further refinement of the operating space. Because of evaporative cooling during drying of the liquid droplets, the droplet temperature is initially much lower than the drying gas temperature; the key criterion for avoiding thermal damage is to maintain the outlet temperature (T_{out}) below some threshold temperature (T_{max}).

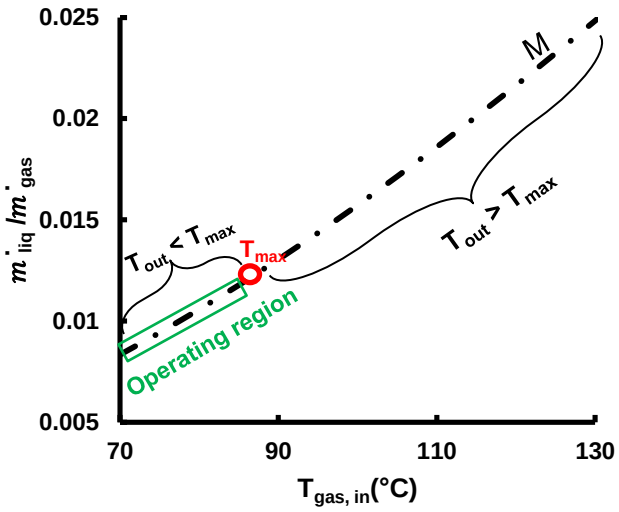

Fig. 6 Representative model predictions for an adiabatic process, illustrating selection of safe operating region for RBC spray drying. See text for details.

To enable the use of the mathematical model to guide design of the spray drying process, it was first necessary to define the necessary parameters, including the moisture sorption isotherm and the sensitivity of RBCs to thermal damage.

3.2 Moisture Sorption Isotherm

To examine the relationship between relative humidity and residual moisture content, packed RBCs were equilibrated at room temperature in the presence of various saturated salt solutions. We initially determined the residual moisture content of the resulting RBC sample by drying in an oven at 105 °C for 24 h, because this method has been used in several previous studies [9]. However, control experiments using sodium tartrate (a dihydrate crystal with a dry basis moisture content of about 18.6%) revealed that drying at 105 °C may not completely remove water from the sample. The sodium tartrate control exhibited an apparent moisture content of only 13.1% ± 0.2% after drying at 105 °C, indicating incomplete drying. To achieve more complete drying, we investigated drying at 150 °C for 3 h. This method yielded a moisture content of 18.8% ± 0.1% for sodium tartrate, which approximately matches the expected value. To further compare these methods, experiments were performed using RBC samples that had been equilibrated at relative humidities of 6.5% and 75%. As shown in Fig. 7, drying at 105 °C resulted in lower apparent moisture content than drying at 150 °C, consistent with the results for the sodium tartrate control samples. In particular, the difference between the moisture content values was statistically

significant for a relative humidity of 6.5% (p = 0.0127). Therefore, drying at 150 °C was used in subsequent experiments to determine the moisture sorption isotherm.

The moisture sorption isotherm for RBCs is shown in Fig. 7. As expected, the equilibrium moisture content of the RBC samples decreased as relative humidity decreased. The data exhibited excellent agreement with the best-fit GAB model (R^2 = 0.996), yielding the following model parameters: M_m = 0.090, C = 21.4, and K = 0.82.

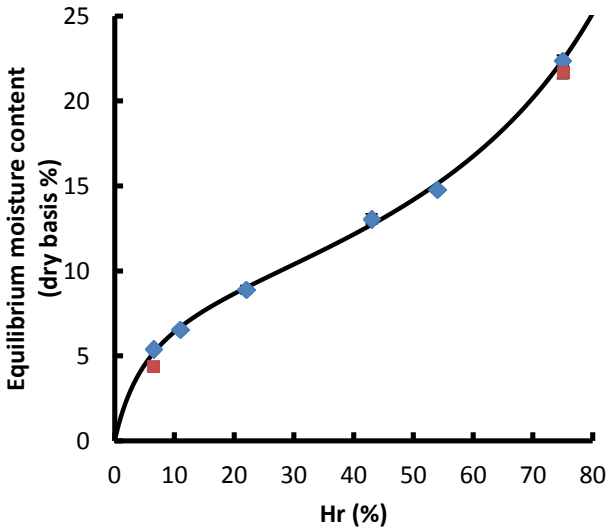

Fig. 7 Moisture sorption isotherm for packed RBCs at room temperature. Equilibrium moisture content was measured by drying at 150 °C for 3 h (diamonds) or by drying at 105 °C for 24 h (squares). The line shows the best fit GAB model (Eq. 1) to data obtained using the 150 °C drying method. Each data point represents the average of 3 replicates.

3.3 RBC Sensitivity to Elevated Temperatures

Fig. 8 displays the hemolysis incurred after brief (25 s) exposure to elevated temperatures between 37 °C and 80 °C. As expected, hemolysis increased as temperature increased, reaching 90 ± 8.4% after exposure to a temperature of 70 °C.

The effect of exposure temperature on hemolysis was statistically significant ($p < 0.0001$) and pairwise comparisons revealed a significant increase in hemolysis for exposure to temperatures of 70 °C or higher, in comparison to the 37 °C control. Surprisingly, the measured hemolysis was lower after exposure to 80 °C (60 ± 8.4%) than 70 °C (90 ± 8.4%), and this difference was statistically significant. We hypothesized that this apparent drop in hemolysis was caused by hemoglobin aggregation and a concomitant decrease in detection of free hemoglobin by spectrophotometry.

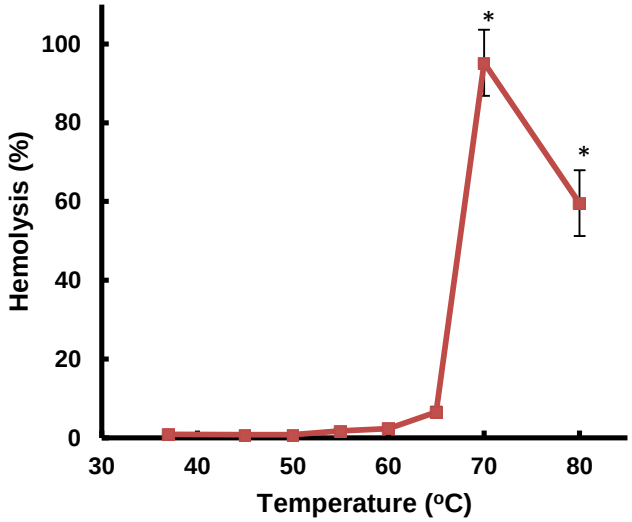

Fig. 8 RBC hemolysis after brief (25 s) exposure to elevated temperatures. Each data point represents the average of 5 replicates. Asterisks indicate a significant difference compared with the 37 °C control.

To investigate this possibility, we performed a series of control experiments in which RBCs were lysed using pure water and exposed to the same temperature conditions. The results of these experiments are shown in Fig. 9. All of the resulting hemolysis values were approximately 100%, with the exception of the sample that had been exposed to 80 °C. In this case, the measured hemolysis was 80.8 ± 4.35%,

significantly lower than the hemolysis values for the other temperatures ($p < 0.05$). This result is consistent with the apparent drop in hemolysis at 80 °C shown in Fig. 8. Together, the results in Figs. 8 and 9 suggest that hemoglobin aggregation prevents accurate measurement of hemolysis after exposure to 80 °C, but not for temperatures of 70 °C and below.

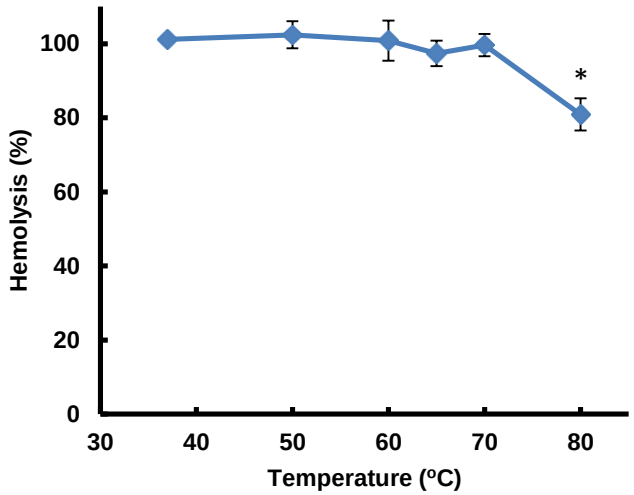

Fig. 9 – Apparent hemolysis after brief exposure of 100% lysed RBCs to elevated temperatures. Each data point represents the average of 3 replicates. The asterisk indicates a significant difference compared with the 37 °C control.

To corroborate the hemolysis data shown in Fig. 8, we also measured cell recovery by counting the number of intact RBCs on a hemacytometer. As shown in Fig. 10, cell recovery remained high (>88%) after exposure to temperatures up to 60 °C. However, cell recovery dropped below 80% and to zero for exposure to 65°C and 70 °C, representing a statistically significant decrease compared with the 37 °C control.

The cell recovery results are also consistent with the evidence in Figs. 8 and 9 suggesting that hemoglobin aggregation occurs after exposure to 80 °C. Obvious

protein aggregation was observed in images of the sample that had been exposed to 80 °C, making accurate quantification of cell recovery impossible. In contrast, images of the sample that had been exposed to 70 °C were clear and did not contain any visible hemoglobin aggregates or intact RBCs.

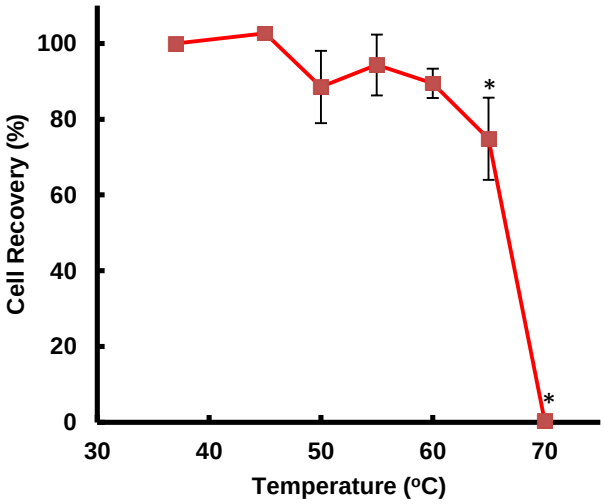

Fig. 10 Recovery of intact RBCs after brief exposure to elevated temperatures. Each data point represents the average of 3 replicates. Asterisks indicate a significant difference compared with the 37 °C control.

3.4 Stability of Trehalose-Loaded RBCs

Based on previous studies of RBC freeze drying [6], we initially planned to evaluate the feasibility of RBC spray drying using trehalose as lyoprotectant. However, before initiating spray drying studies, we first determined the stability of trehalose loading. The results of these experiments are shown in Fig. 11. Substantial hemolysis (28.4%) was observed when the cells were washed twice with isotonic PBS immediately after trehalose loading, and hemolysis continued to rise during storage at 4 °C (green line), reaching 39.9% after 4 h and 46.4% after 24 h. The effect of storage time on

hemolysis was statistically significant (p = 0.0001), with significant differences in pairwise comparisons as indicted in Fig. 11. On the other hand, control RBCs (red line) exhibited hemolysis values that consistently remained less than 1% throughout 24 hours.

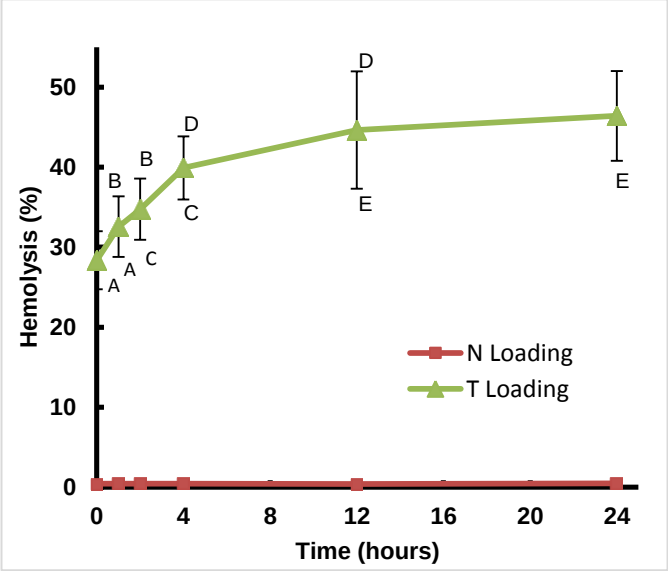

Fig. 11 Stability of RBCs after trehalose loading (green line) compared with control RBCs in isotonic buffer (red line). Each data point represents the average of 3 replicates. Data points with distinct superscript letters are statistically different.

3.5 Spray Drying of RBCs

The mathematical model of the spray drying process (Eq. 1-7) was used to identify the region of the operating space that is predicted to yield a sufficiently dry RBC powder without exposure to excessive temperatures. We selected a target moisture content in the dried RBC powder of $0.05 < M < 0.10$ based on a previous study of RBC freeze drying, which shows that freeze-dried and rehydrated RBCs exhibit an increase in hemolysis when the moisture content is reduced below 0.05 [6]. To avoid thermal damage, the target temperature at the drying chamber outlet was $T_{out} < 65$ °C.

Initially, we made predictions assuming that the drying chamber was adiabatic ($\dot{Q} = 0$). As shown in Fig. 12, the region between the dashed lines for 5% and 10% moisture content defines the inlet conditions that are predicted to yield the target moisture content in the RBC powder. The solid line shows the combinations of inlet conditions that are predicted to yield the threshold outlet temperature of 65 °C; the region to the left of this line is the safe region where $T_{out} < 65$ °C. Therefore, the operating space for RBC spray drying consists of the region between the dashed lines and to the left of the solid line.

To experimentally investigate RBC spray drying we initially used the inlet conditions defined by the red circle in Fig. 12. This corresponds to an inlet drying gas temperature $T_{gas,in}$= 95 °C and a flow rate ratio $\dot{m}_{liq}/\dot{m}_{gas} = 0.021$. This flow rate ratio was achieved using an RBC suspension (at 5% *Hct* with isotonic saline) feed rate $\dot{m}_{liq}$ = 1 g/min and a drying gas (nitrogen) feed rate $\dot{m}_{gas}$ = 46 g/min. Assuming an adiabatic process, these inlet conditions are predicted to yield an outlet temperature of 50 °C and a moisture content of 10%, which corresponds to a relative humidity of 28%. However, experimental measurements deviated substantially from these predictions. The measured temperature at the outlet was only ~28 °C and the measured relative humidity was 70%, indicating substantial loss of heat in the drying chamber.

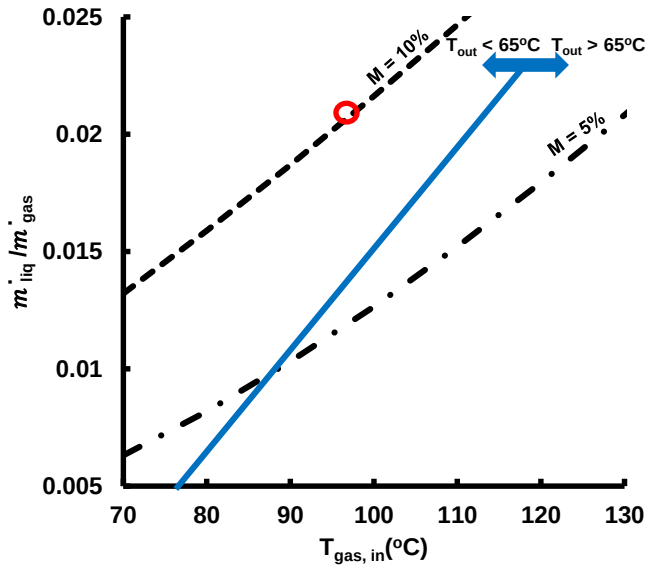

Fig. 12 – Adiabatic spray dryer thermodynamic operating space ($\dot{Q} = 0$)

Therefore, we refined our mathematical model to account for heat loss from the drying chamber. To model the heat transfer process, the drying chamber was divided into two separate control volumes, as illustrated in Fig. 13. In the first control volume, chemical and thermal equilibrium was assumed to occur rapidly, without any heat loss to the surroundings. This allowed the temperature at the outlet of the first control volume to be determined using the Eqs. 1-7 with $\dot{Q} = 0$. In the second control volume, heat loss was assumed to occur but evaporation was neglected. This allowed the heat loss to be modeled using the equation for a heat exchanger:

$$\dot{Q} = UA\left(\frac{(T_{inter} - T_{room}) - (T_{out} - T_{room})}{\ln\left(\frac{T_{inter} - T_{room}}{T_{out} - T_{room}}\right)}\right) \quad 10$$

where T_{room} and T_{inter} are the room temperature and the intermediate temperature after the first control volume, U is the overall heat transfer coefficient and A is the surface area of the chamber.

This modeling approach is justified for the following reasons. From previous computational fluid dynamics (CFD) research, single pass spray dryers have a quite uniform temperature in the whole chamber; however, a significant temperature drop displays at the entrance [13, 40]. Based on the gas inlet flow rate, the residence time of the powder should be at least 1 minute, whereas only a few seconds is typically needed for drying [41]. Thus, having the first control volume containing the water evaporation process and the second control volume accounting for heat loss is a reasonable strategy.

To quantify the overall heat transfer coefficient for our drying chamber, a spray drying experiment was performed using RBC-free saline solutions as the liquid feed. By knowing all the input parameters and the output conditions, the heat transfer coefficient $U = 168\ \frac{J}{s \cdot m^2 \cdot ℃}$ (on average of two experiments).

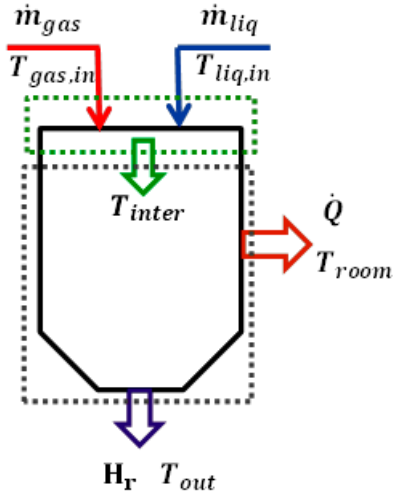

Fig. 13 – The non-adiabatic spray drying chamber involving two separate control volumes ($\dot{Q} \neq 0$)

Fig. 14 displays the new operating space for the non-adiabatic system. In this case, it is relatively easy to achieve the target moisture content ($0.05 < M < 0.10$) while keeping the outlet temperature less than 65 °C. To experimentally investigate RBC spray drying we selected the inlet conditions defined by the red circle: $T_{gas,in}$= 100 °C and $\dot{m}_{liq}/\dot{m}_{gas} = 0.0098$. This flow rate ratio was achieved using an RBC suspension feed rate $\dot{m}_{liq}$ = 0.45 g/min and a drying gas feed rate $\dot{m}_{gas}$ = 46 g/min. These inlet conditions are predicted to yield an outlet temperature of ~32 °C, a residual moisture content in the RBC powder of ~10% and an outlet relative humidity of ~28%.

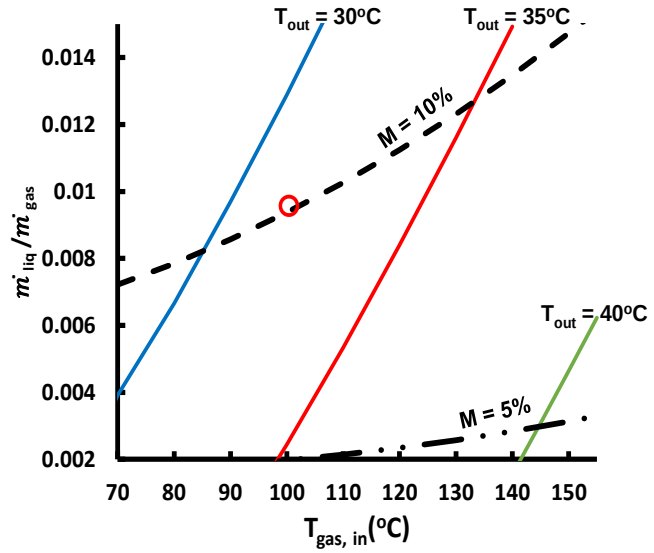

Fig. 14 – Non-adiabatic spray dryer thermal dynamics operating space

Upon initiation of spraying, blood powder was not smoothly generated but a cylindrical shell of solid material accumulated at the nozzle. The shell did not clog the nozzle and after an initial period the shell stopped building up and the powder was generated continuously. After the experiment had finished, visible blood powder

appeared on the filter paper (Fig. 15a). The experimentally measured outlet temperature was 32.3ºC and the measured relative humidity was 28.0% on average (Table 4). Measurements of the moisture content of the RBC powder yielded an average of 10.5% after the spray-dried RBCs powder was scratched down carefully from the filter paper (Fig. 15b), and then placed in oven at 150°C for 3 hours. These results approximately match the predicted outlet conditions.

Table 2 Spray drying input parameters and results

Run	Relative Humidity (%)	Output Temperature (°C)	Residual Moisture Content from oven(%)
1	26.6	33.0	14.7*
2	30.7	31.3	9.35
3	26.6	32.7	7.59
Avg	28.0	32.3	10.5

*Measurement collected at one week after spray drying experiment

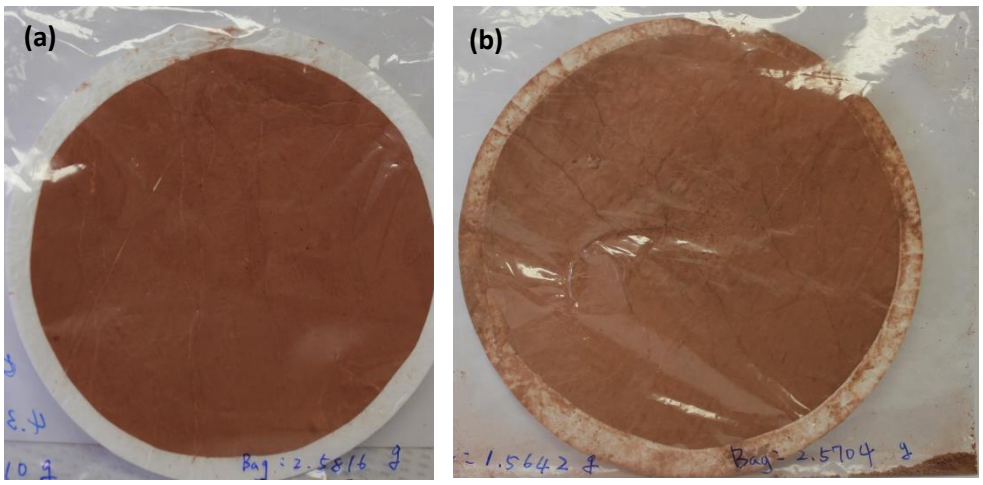

Fig. 15 – (a)RBCs on filter paper after spray drying before scratching (first batch of blood); (b) RBCs on filter paper after spray drying after scratching (second batch of blood)

The spray-dried RBCs had been rehydrated with PBS as well. Fig. 16 shows the trehalose-loaded RBCs (tRBCs) under different circumstances. Fig. 16a displays tRBCs before being spray-dried; no protein aggregates were observed under the

microscope; Fig. 16b and c diplay potentially viable tRBCs after PBS rehydration (from two different batches). However, protein aggregates prevent accurate measurement of hemolysis by spectrophotometry. Therefore, only a qualitative anlaysis could be done at this point.

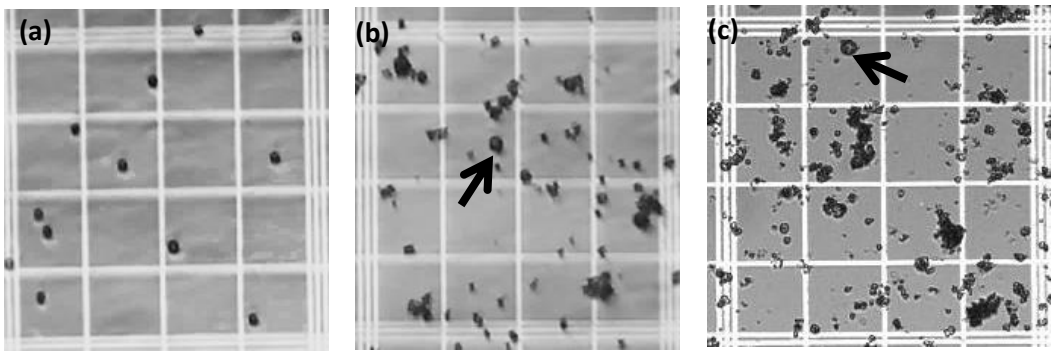

Fig. 16 – Trehalose-loaded RBCs microscopic view. (a)tRBCs without spray drying; (b) and (c) Spray-dried tRBC after PBS rehydration (two different batches of blood)

CHAPTER4: Discussion

4.1 Moisture Sorption Isotherm

The sorption curve in Fig. 3 shows a sigmoidal shape, consistent with the sorption curves generated in previous food science studies [28] and studies involving yeast [29] and human platelets [30]. The curve shape in Fig. 3 is consistent with the shape of a curve demonstrating Type II sorption (one of the 5 types of sorption established in Brunauer et al.[42]). In addition, the GAB model used by Bruanauer et al. for Type II sorption properly matches the data generated in our study as well.

4.2 RBCs Sensitivity to Elevated Temperatures

In order to successfully achieve moisture content of 5% in dried RBC powder, the evaporation of moisture from the atomized RBCs must take place quickly, which requires a high temperature gas. Fildes et al. concluded that RBCs could withstand temperatures of 60^{o}C for 0.6 seconds without displaying significant hemolysis or osmotic damage [17]. 0.6 seconds is also an ideal amount of time in which to complete the moisture evaporation. Our own experiments have shown that RBCs can withstand 25-second exposure at 65^{o}C (which we determined as the threshold temperature for 25 second exposure) with acceptable levels of hemolysis. Although hemolysis levels were acceptable, cell recovery tests show instability resulting from thermal shock. Fildes et al. also found osmotic fragility was caused at lower temperatures than hemolysis [18], so further study on damage occurring at lower temperature exposures is suggested.

4.3 Stability of Trehalose-Loaded RBCs

Intracellular trehalose loading has been demonstrated to increase survivability of cells during the freeze drying process [6]. Recent studies have achieved better than 90% recovery of human platelets when loaded with trehalose [14, 24], demonstrating trehalose's ability as a lyoprotectant. On the other hand, the trehalose loading process is known to cause cellular damage due to Hb oxidation and membrane lipid peroxidation [27], and the transfer of the trehalose loaded RBCs from the hypertonic trehalose loading buffer into a physiologically isotonic solution results in cell damage [26]. Our results in Fig. 11 show 28% hemolysis after 7 hours of trehalose loading

and two washes with isotonic saline, which is essentially identical to the results found by Satpathy et al. (which show hemolysis of 10% and 19% caused by the loading and resuspension process, respectively) [26]. Most previous studies on treshalose loading focused only on hemolysis occurring during the loading process or shortly after. During our study, we found an additional 12% hemolysis occurring by 4 hours post resuspension with isotonic saline, and 16% additional hemolysis occurring by 12 hours post resuspension. Because of this, we recommend the resuspended solution should be refrigerated for 4 hours (until the remaining RBCs are more stable) before conducting further analysis (such as spray drying experiments).

4.4 Spray Drying of RBCs

4.4.1 Observation of Spray Drying

Due to much heat loss, we found that a non-adiabatic model predicted experimental operating parameters much more accurately. During the spray drying experiment dried RBC powder was generated, but a cylindrical dried-blood 'shell' was observed forming at the nozzle. As the solution flowed through the nozzle, the hot nitrogen gas dried the RBC solution quick enough that dried RBCs began to accumulate at the nozzle before atomization even took place. As a result, the 'shell' also changes the geometry of the nozzle, which may result in spraying behavior inconsistent with that designed by the manufacturer. In order to keep our experiment consistent with that of the manufacturing design as well as McLean et al. study [24], we must work to eliminate the build up of this dried-blood 'shell' at the nozzle.

4.4.2 Observation of Rehydration

After rehydration of the dried RBC powder, many protein aggregates and few intact RBCs were observed under the microscope. We hypothesize that the low amount of intact RBCs is a result of shear-induced damage. According to the McLean et al. study, high gas-to-liquid flow rate ratios result in higher hemolysis [24]. McLean et al. found an approximate 5% hemolysis when using a (10 L/min)/(1 mL/min) gas-to-liquid flow rate ratio with a 3% hematocrit solution, whereas the flow rate ratio of 20/1 at the same hematocrit resulted in 15% hemolysis [24]. However, even their highest experimental gas-to-liquid flow rate ratio (20/1) was much lower than the gas-to-liquid flow rate ratio used in our experiment (~50/0.45). The reason we were unable to replicate the gas-to-liquid flow rate ratios used by McLean et al. is because of the constraints of the non-adiabatic model, which required a higher gas-to-liquid flow rate ratio in order to adequately dry the sample. It is also worth mentioning that the adiabatic-model also required a higher gas-to-liquid flow rate ratio than what was used by McLean et al. It is therefore necessary to build a secondary gas inlet with which we can provide an adequate amount of gas to dry the sample while at the same time lowering the shear stresses felt by the RBCs at the nozzle. As the gas-to-liquid flow rate at the nozzle approaches the ratios used in the McLean et al. study, we expect shear-induced damage to be reduced and 'shell' generation to be eliminated. Besides mitigating damage to the RBCs by changing the experimental parameters, chemical protectants may also be used to protect the RBCs against damage. The extracellular protectant, human serum albumin, has been demonstrated to protect

RBCs during freeze drying [5, 6]. Investigating the use of human serum albumin or other extracellular protectants may be worthwhile in future studies.

4.4.3 Model Evaluation

Our experimental results quantitatively show the accuracy of our model prediction. The experimental value of T_{out} displayed less than 1% difference from the predicted value, which is a fairly accurate result. The average experimentally measured relative humidity differed from the predicted value by less than 0.1%, further demonstrating the accuracy of the model. The value of *M* differed from the model prediction by ~5%. Since the oven desiccation has a process of powder collection and powder quantification, the powder might be slightly moisturized during the process. Therefore, it is understandable that the oven desiccation might provide a larger error while transferring the powder from the filter paper to the oven.

CHAPTER 5: Conclusions and Future Directions

In summary, preliminary experiments were done first in order to create the boundary of our mathematical model. Our completed mathematical model suggested operating parameters, and the experimental results were used to evaluate the accuracy of our model. In preliminary experiments, the GAB model was found to fit the curve generated by our moisture sorption isotherm experiment, allowing us to accurately use the model for *Hr* between 0% and 70%. We determined that 25-second exposure of RBCs at 65^{o}C does not cause significant hemolysis. We also determined that post-

trehalose-loaded RBCs should be stored in refrigeration for 4 hours (until the solution is more stable with time) before conducting further analysis or running the spray drying experiment.

Our spray drying device allowed us to generate powder with ~10% water content even in non-adiabatic conditions although chamber insulation needs to be improved. Analysis indicates that some intact RBCs were generated after rehydration but aggregation must be reduced. Creating a secondary gas input is a possible way to reduce shear-induced damage while it would let us use the same gas-to-liquid flow ratios at the nozzle that the McLean et al. study provided [24]. In addition to intracellular lyoprotectants, extracellular lyoprotectants may provide another way by which to decrease shear-induced damage since it is proven to stabilize the RBC membrane [5,6]

Bibliography

1. *Report of the US Department of Health and Human Services. The 2011 national blood collection and utilization survey report*. 2013, Washington, DC: US Department of Health and Human Services, Officeof the Assistant Secretary for Health.
2. Lecak, J., K. Scott, C. Young, J. Hannon, and J.P. Acker, *Evaluation of red blood cells stored at-80 degrees C in excess of 10 years.* Transfusion, 2004. **44**(9): p. 1306-1313.
3. Holovati, J.L., K.A. Wong, J.M. Webster, and J.P. Acker, *The effects of cryopreservation on red bloodcell microvesiculation, phosphatidylserine externalization, and CD47 expression.* Transfusion, 2008.**48**(8): p. 1658-68.
4. Valeri, C.R. *Standard Operating Procedure. Glycerolization and Deglycerolization of Red Blood Cells in a Closed System Using the Haemonetics ACP215. Retrieved October 1, 2011*. [cited 2011 October 1]; Available from: www.nbrl.org/SOP/ACP215.
5. Kheirolomoom, A., G.R. Satpathy, Z. Torok, M. Banerjee, R. Bali, R.C. Novaes, E. Little, D.M. Manning, D.M. Dwyre, F. Tablin, J.H. Crowe, and N.A. Tsvetkova, *Phospholipid vesicles increase the survival of freeze-dried human red blood cells.* Cryobiology, 2005. **51**(3): p. 290-305.
6. Torok, Z., G. Satpathy, M. Banerjee, R. Bali, E. Little, R. Novaes, H. Ly, D.M. Dwyre, A. Kheirolomoom, F. Tablin, J.H. Crowe, and N.M. Tsvetkova, *Preservation of trehalose-loaded red blood cells by lyophilization.* Cell Preservation Technology, 2005. **3**(2): p. 96-111.
7. Booth, G.S., J.N. Lozier, K. Nghiem, D. Clibourn, H.G. Klein, and W.A. Flegel, *Spray: single-donor plasma product for room temperature storage.* Transfusion, 2012. **52**(4): p. 828-33.
8. Ananta, E., M. Volkert, and D. Knorr, *Cellular injuries and storage stability of spray-dried Lactobacillus rhamnosus GG.* International Dairy Journal, 2005. **15**(4): p. 399-409.

9. Sunny-Roberts, E.O., Knorr, D, *The protective effect of monosodium glutamate on survival of Lactobacillus rhamnosus GG and Lactobacillus rhamnosus E-97800 (E800) strains during spray-drying and storage in trehalose-containing powders*. International Dairy Journal, 2009. **19**(4): p.209-214.

10. Kanias, T. and J.P. Acker, *Mechanism of hemoglobin-induced cellular injury in desiccated red blood cells*. Free Radical Biology and Medicine, 2010. **49**(4): p. 539-547.

11. Chakraborty, N., D. Biswas, and G.D. Elliott, *A Simple Mechanistic Way to Increase the Survival of Mammalian Cells During Processing for Dry Storage*. Biopreservation and Biobanking, 2010. **8**(2): p. 107-114.

12. Sitaula, R., J. Jimenez, and S. Bhowmick, *Osmotic Damage as a Predictor of Motility Loss During Convective Desiccation of Bovine Sperm*. Biopreservation and Biobanking, 2013. **11**(6): p. 371-378.

13. Mezhericher, M., Levy, A., Borde, I. *Spray drying modelling based on advanced droplet drying kinetics*. Chemical Engineering and Processing: Process Intensification, 2010. **49**(11): p.1205-1213.

14. Crowe, J.H., F. Tablin, W.F. Wolkers, K. Gousset, N.M. Tsvetkova, and J. Ricker, *Stabilization of membranes in human platelets freeze-dried with trehalose*. Chemistry and Physics of Lipids, 2003. **122**(1-2): p. 41-52.

15. Coakley, W.T., A.J. Bater, L.A. Crum, and J.O.T. Deeley, *Morphological-Changes, Hemolysis and Microvesicularization of Heated Human-Erythrocytes*. Journal of Thermal Biology, 1979. **4**(1): p. 85-93.

16. Gershfeld, N.L. and M. Murayama, *Thermal-Instability of Red Blood-Cell Membrane Bilayers - Temperature-Dependence of Hemolysis*. Journal of Membrane Biology, 1988. **101**(1): p. 67-72.

17. Ivanov, I.T., *Thermohemolysis of Human Erythrocytes in Sucrose Containing Isotonic Media*. Journal of Thermal Biology, 1992. **17**(6): p. 375-379.

18. Fildes, J., S. Fisher, C.M. Sheaff, and J.A. Barrett, *Effects of short heat exposure on human red and white blood cells*. Journal of Trauma, 1998. **45**(3): p. 479-84.

19. Lepock, J.R., H.E. Frey, H. Bayne, and J. Markus, *Relationship of Hyperthermia-Induced Hemolysis of Human-Erythrocytes to the Thermal-*

Denaturation of Membrane-Proteins. Biochimica Et Biophysica Acta, 1989. **980**(2): p. 191-201.

20. Ho, K.C. and P.S. Lin, *Response of Erythrocytes to Heat in the Presence of D2o, Glycerol, and Anisotonic Saline*. Radiation Research, 1991. **125**(1): p. 20-27.

21. Di Domenico, R. and R. Lavecchia, *Thermal stability of human haemoglobin in the presence of sarcosine and sorbitol*. Biotechnology Letters, 2000. **22**(5): p. 335-339.

22. Wolkers, W.F., N.J. Walker, F. Tablin, and J.H. Crowe, *Human platelets loaded with trehalose survive freeze-drying.* Cryobiology, 2001. **42**(2): p. 79-87.

23. Masters, K. *The Spray Drying Handbook*. Essex [England]: Longman Scientific & Technical; New York: John Wiley, 1991.

24. McLean, M., X.Y. Han, and A.Z. Higgins, *Spray Drying for Preservation of Erythrocytes: Effect of Atomization on Hemolysis*. Biopreservation and Biobanking, 2013. **11**(2): p. 122-123.

25. Conrad, P.B., Miller, D.P., Cielenski, P.R., and de Pablo, J.J. *Stabilization and preservation of Lactobacillus acidophillus in saccharide matrices*. Cryobiology, 2000. **41**(1): p17-24.

26. Satpathy, G.R., Z. Torok, R. Bali, D.M. Dwyre, E. Little, N.J. Walker, F. Tablin, J.H. Crowe, and N.M. Tsvetkova, *Loading red blood cells with trehalose: a step towards biostabilization.* Cryobiology, 2004. **49**(2): p. 123-36.

27. Kanias, T. and J.P. Acker, *Trehalose loading into red blood cells is accompanied with hemoglobin oxidation and membrane lipid peroxidation.* Cryobiology, 2009. **58**(2): p. 232-239.

28. Andrade P., R.D., Lemus M., R., E. Perez C., C., Models of sorption isotherms for food: uses and limitations. VITAE, 2011, **18**(3): p. 325-334.

29. Koga, S., Echigo, A., Nunomura, K., *Physical properties of cell water in partially dried Saccharomyces cerevisiae*. Biophysical Journal, 1996. **6**(5): p.665-675.

30. Xu, M., Chen, G., Fan, J., Liu, J., Xu, X., Zhang, S., *Moisture sorption characteristics of freeze-dried human platelets.* Jzus, 2011. **12**(3): p.210-218.

31. Felder, R.M., Rousseau, R.W., *Elementary Principles of Chemical Process 3rd Edition*, John Wiley &Sons, Inc., Hoboken, NJ, 2005, pp 641-643

32. Nuess, J.D., O'Brien, M.G., Frediani, H.A., *Sodium tartrate dehydrate as a primary standard for Karl Fisher reagent*. Chemical Control Division, Merck &Co., Inc., Rahway, NJ, 1951. **23**(9): p. 1332-1333.

33. Han, V., K. Serrano, and D.V. Devine, *A comparative study of common techniques used to measure haemolysis in stored red cell concentrates.* Vox Sanguinis, 2010. **98**(2): p. 116-23.

34. Lusianti, R.E., Benson, J.D., Acker, J.P., Higgins, A.Z., *Rapid removal of glycerol from frozen-thawed red blood cells.* Biotechnology Progress, 2013. **69**: p.609-620.

35. Yan, Y-B., Wang, Q., He, H-W, Zhou, H-M, *Protein Thermal Aggregation Involves Distinct Regions: Sequential Events in the Heat-Induced Unfolding and Aggregation of Hemoglobin.* Biophysical Journal, 2004. **86**: p.1682-1690.

36. Alexander, R. W., Schlant, R. C., and Fuster, V. *'Hurst's the Heart, Arteries and Veins*. 9th Edition Mc Graw-Hill, New York, NY. 1998.

37. Beilin, L.J., Knight, G.J., Munro-Faure, A.D., Anderson, J., The sodium, potassium, and water content of red blood cells of healthy human adults. Journal of Clinical Investigation, 1966. **45**(11): p.1817-1825.

38. Maltesen, M.J, Bjerregaard, S., Hovgaard, L., Havelund, S., Weert, M., *Quality by design – Spray drying of insulin intended for inhalation*. European Journal of Pharmaceutics and Biopharmaceutics, 2008. **78**: p.825-838.

39. Prinn, K.B., Costantino, H.R., Tracy, M., *Statistical modeling of protein spray drying at the lab scale*. AAPS PharmSciTech, 2002. **3**(1): article 4.

40. Dorby, D.R., Settell, D.M., Baumann, J.M., Ray, R.J., Graham, L.J., Beyerinck, R.A., *A model-based methodology for spray-drying process development.* Journal of Pharmaceutical Innovation, 2009. **4**(3): p.133-142.

41. Zbicinski, I., Delag, A., Strumillo, C., Adamiec, J., *Advanced experimental analysis of drying kinetics in spray drying.* Chemical Engineering Journal, 2002. **86**(1): p.207-216.

42. Brunauer, S., Deming, L.S., Teller, E., *On a theory of Vander Waals adsorption of gases*. J Am Chem Soc, 1940. **62**(7): p.1723-1732.

Appendix

A.1 Isotonic Saline Protocol

Materials

8.3	g	Sodium Chloride, NaCl
1.77	g	Disodium phosphate, Na_2HPO_4
2	g	Glucose
1	L	Ultrapure H2O
		2 N HCl and 2 N NaOH
		Sterile bottle top filter, 500 mL
		Sterile bottle, 1 L
		Beaker, 1 L
		Graduated clylinder, 1 L
		Stir bar
		Stir plate
		Parafilm
		Osmometer tips

Procedure

1. Place stir bar inside beaker and set on stir plate.
2. Measure 1 L of ultrapure water using graduated cylinder and dispense into beaker.
3. Weigh the sodium chloride, disodium phosphate, glucose and add it into the beaker.
4. Start the stir function on the stir plate and continue until all salt are visibly dissolved. While stirring, turn on the osmometer
5. Once salts are all dissolved adjust the pH to 7 by dropwise addition of NaOH or HCl.
6. Take a sample of the solution and measure the osmolality with the osmometer.
7. Once the right osmolality is attained, stop the stir function and cover the beaker with parafilm.
8. Sanitize bottle and attach bottle top filter and vacuum.
9. Process saline solution into sterile bottle.
10. Cap and label the bottle appropriately, place in the refrigerator.

A.2 Trehalose Loading Procedure

(taken from Satpathy et. al. 2004)

1. The loading buffer contains 800 mM trehalose, 100 mOsm ADSOL, and 6.7 mM potassium phosphate (pH 7.2). ADSOL can be made in a 462 mOsm stock solution containing 111 mM glucose, 2 mM adenine, 154 mM NaCl, and 41 mM mannitol in an aqueous solution.

2. Take whole blood and centrifuge at 1800g for 10 min. Remove plasma so only red blood cells remain. Then wash 3 times in 1X PBS for 5 min in the centrifuge at 1800g. Remove the PBS after the final centrifugation and add the loading buffer such that the sample is at 30% hematocrit. Shake the solution until the blood cells are well mixed in the loading buffer.

3. Incubate the RBC in the trehalose buffer at 37 degrees for 7 hours.

4. After incubation, centrifuge the sample at 1800g for 5 minute and remove the loading buffer. Wash the loaded blood three times with 1X PBS. Then place the loaded RBC in PBS for storage at 4 degrees Celsius until ready to use.

A.3 Spray Drying Enclosure Design

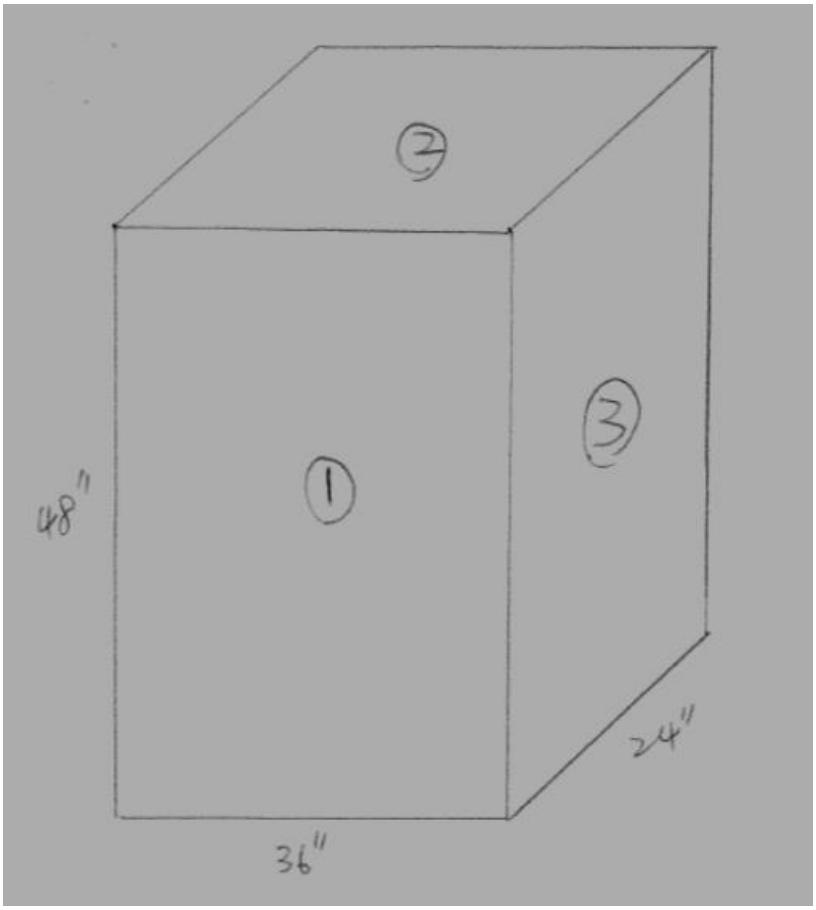

A.3 Spray Drying Enclosure Design (continue)